Electrical Signature Analysis for Condition Monitoring of Permanent Magnet Synchronous Machine

Camila Paes SALOMON[1], Claudio FERREIRA[1], Germano LAMBERT-TORRES [2],
Carlos Eduardo TEIXEIRA[1], Luiz Eduardo BORGES DA SILVA[1],
Wilson Cesar SANTANA[2], Erik Leandro BONALDI[2], Levy Ely de Lacerda DE OLIVEIRA[2]
[1]*Itajuba Federal University, UNIFEI, Itajuba, MG, 37500-903, Brazil*
[2]*Gnarus Institute, Itajuba, MG, 37500-052, Brazil*
germanoltorres@gmail.com

***Abstract*—Permanent magnet synchronous machines (PMSMs) drives are attractive and have been used in several applications, because of their noteworthy advantages. In some applications, the continuous operation is necessary, and then the PMSM drive outage is unacceptable or may cause great losses. Thus, several studies have been accomplished in order to detect incipient faults in PMSMs. In this context, the electrical signature analysis (ESA) technique is highlighted, because of the feasibility and non-invasive features. ESA allows the fault detection by only analyzing the electrical machine quantities. This paper proposes a study of ESA for PMSM condition monitoring. The review of some fault patterns is presented as well as the development of a scale model laboratory to simulate faults in a real PMSM in operation. The PMSM is used to drive a fluid pumping system, and different types of fluids are tested, being different load conditions from the PMSM point of view. The presented results are promising, encouraging ESA based methodologies for PMSM fault detection.**

***Index Terms*—condition monitoring, digital signatures, fault detection, permanent magnet machines, predictive maintenance.**

I. INTRODUCTION

Permanent magnet synchronous machines (PMSMs) are attractive and have been used in several applications, as hybrid electric vehicles; aircraft; nuclear power plants; submarines; robotic applications; medical and industrial servo drives; and distributed generation applications. These machines have been increasingly used in variable speed and high-performance electric drives, because of their advantages as simple construction; high efficiency; high power density; high power factor; precise torque control; and wide speed range with constant power.

In some applications, the continuous operation is necessary, so an outage in the PMSM drive is unacceptable or may cause great losses [1-3]. Because of the aforementioned reasons, several studies have been accomplished focusing on early fault detection in PMSMs or fault tolerant PMSM drives [4].

Among the strategies that have been used for PMSMs fault detection, the predictive maintenance (PdM) is highlighted. This type of maintenance uses techniques to assess the equipment in order to decide what and when the maintenance action should be done. For such purpose, in general, some parameters related to the condition of the machine are continuously monitored in order to evaluate if certain indicators present signs of decreasing performance or incipient fault.

One of the techniques used in PdM is electrical signature analysis (ESA). The monitored parameters in ESA are the electrical signals of the machine, mainly the stator currents. ESA is based on the analysis of the electrical signals frequency spectra, obtained by using Fast Fourier Transform (FFT) and other signal processing procedures. There are frequency components in the spectra whose magnitudes change in the presence of a fault, which are called ESA fault patterns. Thus, the faults can be detected and identified by analyzing these fault patterns. The faults can be detected in early stage, and the severity is related to the component magnitude. Finally, the advantages of ESA include low intrusiveness; technical and economic viability; and dependence on only the electrical signals of the machine [5, 6].

Several works have been published about ESA-based methodologies for fault detection in PMSMs. The works have approached mainly the detection of open phase fault [1, 7]; stator winding inter-turn short circuit [3, 8, 9]; rotor demagnetization [2, 10]; mechanical misalignment; mechanical unbalance [11]; airgap eccentricity [12, 13]; bearing fault [14]; and motor drive faults [15].

This paper presents an approach of ESA for PMSM condition monitoring. The review of some fault patterns found in literature is presented as well as some peculiarities in ESA application for fault detection in these machines. The development of a scale model laboratory to simulate faults in a real PMSM in operation is described, including the fault simulation methodology. The PMSM is used to drive a fluid pumping system, and different types of fluids are tested, which mean different load conditions from the PMSM point of view. The goal is to perform the analysis aiming a future application in PMSM for subsea oil pumping. Finally, preliminary experimental results are presented. The results were promising, encouraging ESA based methodologies for PMSM fault detection.

This work was supported in part by the CNPq – Brazilian National Science Foundation under Grant 303380/2017-9.

Digital Object Identifier 10.4316/AECE.2018.04011

II. Electrical Signature Analysis for Permanent Magnet Synchronous Machines

Electrical signature analysis is a technique used for machine condition monitoring based on the analysis of the electrical signals in the frequency domain. Usually, a FFT algorithm is performed to the signals, and the spectra (or *electrical signatures*) are obtained. The fault detection is performed by analyzing the frequency components of the electrical signatures. There are specific frequencies whose magnitude changes when some faults happen. Each fault excites specific frequency components, which are called *fault patterns*. They are generally dependent on the line frequency and structural characteristics of the machine [5].

The fault patterns are usually expressed in the frequency spectrum as:

$$f_e = f_1 \pm k \cdot f_c \tag{1}$$

where f_e is the frequency of the fault in the spectrum; f_1 is the fundamental frequency (line frequency); k is a positive integer value, indicating the harmonic order; and f_c is characteristic frequency of the fault. Thus, f_c appears as a modulation of the fundamental frequency, whose harmonics are defined by k.

In the case of PMSMs, some faults are emphasized. The faults approached in the present work include stator electrical unbalance (and so open phase, indirectly), mechanical misalignment, and mechanical unbalance. Moreover, the PMSM was used to drive a fluid pumping system, as will be presented in the section III. Thus, it is important to define some relations used in the fault patterns.

Firstly, the rotor rotation frequency (f_r) is given by:

$$f_r = \frac{f_1}{p} \tag{2}$$

where p is the number of pole pairs of the machine.

The gear rotation frequency at pump input ($f_{r\#1}$), considering the speed reducer between the PMSM and the pump, is given by:

$$f_{r\#1} = \frac{f_r}{pump\ reduction\ factor} \tag{3}$$

The gear rotation frequency at pump output ($f_{r\#2}$) is computed considering the number of teeth of the bigger gear (N) and of the smaller gear (n):

$$f_{r\#2} = \frac{N}{n} \cdot f_{r\#1} \tag{4}$$

The gear frequency is defined as:

$$f_{gear} = N \cdot f_{r\#1} = n \cdot f_{r\#2} \tag{5}$$

Thus, the ESA notable frequency components for PMSM considered in this work are presented in the Table I. The mathematical proof for them can be found in [5, 16-18].

Finally, it is important to say that there are some peculiarities in ESA applied to fault detection in PMSMs. They include the characteristic of speed variations and some fault patterns that coincide in the same frequency, which requires study in order to distinguish the faults effects. These peculiarities are not in the scope of the present work.

III. Development of a Scale Model Laboratory

A scale model laboratory has been developed in order to verify and develop ESA fault patterns for PMSM. The main objectives were to operate a PMSM and inject faults in a controlled way. The mid-term goal with this work is to apply the ESA based system to detect faults in PMSMs for subsea oil pumping. Thus, this motivated the type of load chosen in the experimental setup, using the PMSM to drive a fluid pumping system, considering the fluids water, diesel fuel and water plus diesel fuel.

Fig. 1 presents a picture of the scale model laboratory. It basically consists in a system for fluid pumping, in which a PMSM drives a gear pump. The PMSM is driven by a frequency converter, and there is a speed reducer between the PMSM and the pump in order to adjust the speed. The PMSM ratings are: 5 HP, 6 poles, 220 V, 11.8 A, 1200 rpm.

Three types of faults can be injected in the scale model laboratory: stator electrical unbalance; mechanical misalignment; and mechanical unbalance.

The stator electrical unbalance fault is simulated through the insertion of resistors between the frequency converter and the PMSM input (Fig. 2). Two phases are provided with an additional 1 Ω series resistance, and one phase is provided without an additional series resistance, simulating the electrical unbalance. An observation is made in this point. The simulated electrical unbalance is small. Thus, if it is detected in the ESA, it is also valid for the open phase fault detection, which would be a more severe case of electrical unbalance.

TABLE 1. NOTABLE ESA FREQUENCY COMPONENTS FOR PMSM

Item	Related Faults	Theoretical Pattern
Rotor Rotation Frequency	Mechanical misalignment	$f_1 \pm k.f_r$
	Mechanical unbalance	
Gear Rotation Frequency #1 (at pump input)	Gear problem	$f_1 \pm k.f_{r\#1}$
Gear Rotation Frequency #2 (at pump output)	Gear problem	$f_1 \pm k.f_{r\#2}$
Gear Frequency	Gear problem	$f_1 \pm k.f_{gear}$
Third Harmonic	Stator electrical unbalance	$3.f_1$
	Open phase fault	
EPVA (Extended Park's Vector Approach) Electrical Unbalance	Stator electrical unbalance	$2.f_1$ (at EPVA spectrum)
	Open phase fault	

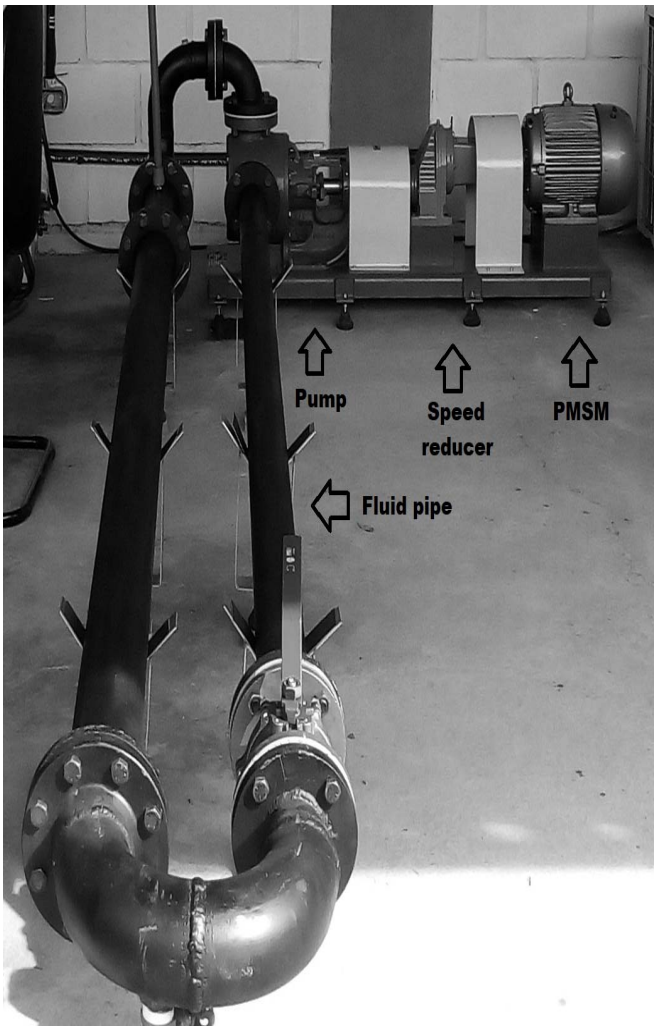

Figure 1. Scale model laboratory

Another simulated fault is mechanical misalignment, which is simulated by inserting four stacked cards between the PMSM base and the PMSM foot at one side of the motor. It causes a misalignment on the machine set. The last simulated fault was mechanical unbalance. This fault was simulated through the insertion of a plastic clamp with four side-by-side screw-nuts on the coupling between the speed reducer and the PMSM. This causes the presence of a concentrated mass in a region of the coupling, generating a mechanical unbalance. Fig. 3 illustrates the simulation of mechanical problems.

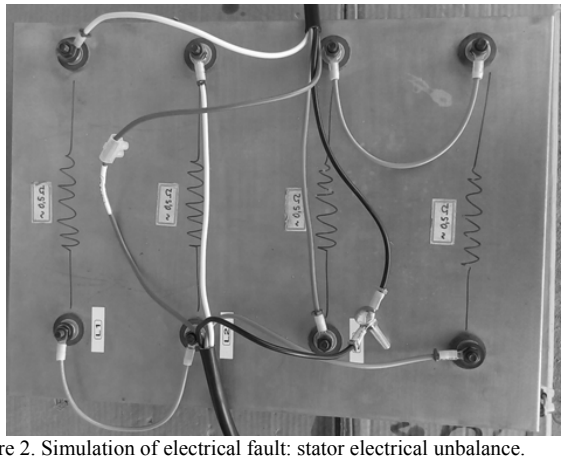

Figure 2. Simulation of electrical fault: stator electrical unbalance.

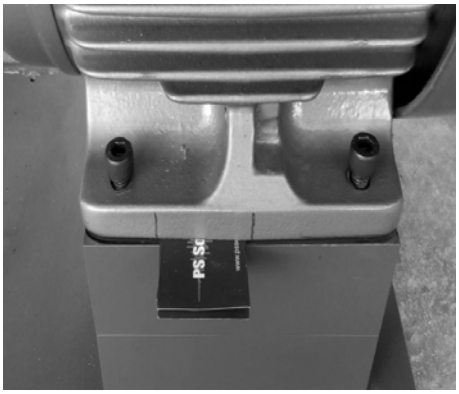

(a)

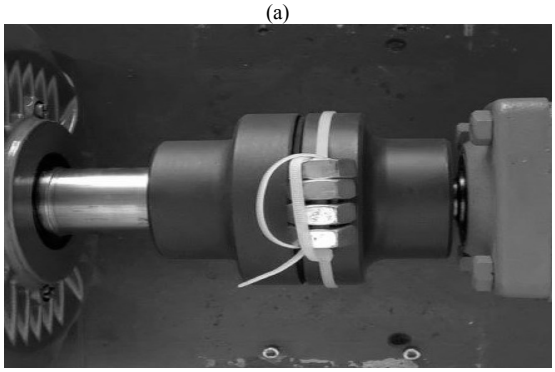

(b)

Figure 3. Simulation of mechanical problems: (a) mechanical misalignment and (b) mechanical unbalance.

The measured data were the three line currents and phase-to-phase voltages at the frequency converter output. The currents and voltages were measured by using potential transformers (PS TTD-0 672X) and current transformers (PS TT 50-SD 33.333 mV/A). The data acquisition was performed through a dedicated hardware (Preditor PR4 – 8 channels, 24 bits), which communicates with a computer, where the signal processing and analysis are accomplished.

IV. Results and Analysis

This section presents the experimental results with the scale model laboratory. The experiments have been accomplished considering three types of fluids being pumped in the scale model laboratory. The analysis is divided in two main goals – first, a comparison among current signals in baseline ("healthy") condition acquired with different types of fluids; and second, the fault simulation results. The analysis was performed with signal length of 40 seconds, acquired with a sampling frequency of 46875 Hz.

A. Differences and Similarities Considering Different Fluids

This item presents the results of comparison among current signals considering the different types of fluids. The main goal of this analysis is to detect differences and similarities among the signals, in order to help in the fluid identification by analyzing the current signals.

Fig. 4 presents the phase A current spectra for the three types of fluids, highlighting some notable frequency components. In Fig. 4, one can note the first sideband of rotation frequency components (black arrows); the first

sideband of gear rotation frequency #1 (at pump input) components (white arrows); and the first sideband of gear rotation frequency #2 (at pump output) components (gray arrows). Considering the line frequency of 50 Hz (used in the tests) and the expressions (2)-(5), the expected values for these frequencies were 16.667 Hz for the rotation frequency; 6.562 Hz for the gear rotation frequency #1; and 9.022 Hz for the gear rotation frequency #2. Then, these components are analyzed around the line frequency of 50 Hz, considering the frequency modulation.

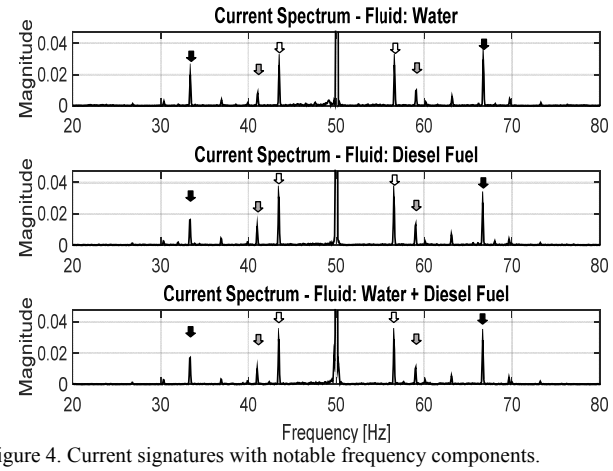

Figure 4. Current signatures with notable frequency components.

From Fig. 4, it can be noted that these components are evident in the spectra, considering the three types of fluids. There is a small turbulence around the line frequency, especially in the cases of water fluid and water plus diesel fuel fluid. This characteristic can help in distinguishing the type of fluid by analyzing the current signals.

Fig. 5 presents the phase A current spectra for the three types of fluids, highlighting the gear frequency pattern region. The expected value for this frequency was 72.178 Hz, corresponding to the first right sideband of 122.178 Hz. It can be noted that these components are in the noise level, indicating that there is no gear problem in the setup.

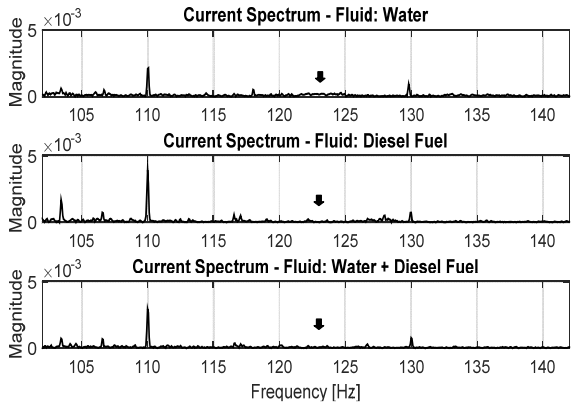

Figure 5. Current signatures – gear rotation frequency pattern region.

B. Fault Simulation Results

This item presents the results of fault simulation for each type of fluid in the pipe. The simulated faults were stator electrical unbalance; mechanical misalignment; and mechanical unbalance. For stator electrical unbalance, the obtained fault patterns were the third harmonic on current signature and the electrical unbalance pattern (two times the line frequency) on EPVA current signature. For mechanical misalignment and mechanical unbalance faults, the obtained fault pattern was the rotation frequency on current signature. The components magnitudes are presented normalized in relation to the fundamental frequency, in linear scale and in dB scale. The latter is common for ESA in the context of PdM, as it allows the comparison of magnitudes with large ranges of differences.

1. Water Fluid

The first analyzed fault is stator electrical unbalance. Figs. 6 and 7 present the current spectra for the third harmonic and EPVA electrical unbalance fault patterns, respectively, considering the baseline and fault conditions. The third harmonic is expected to be close to the 150 Hz frequency component. From Fig. 6, the components magnitudes were 0.00469 (-46.57 dB) for baseline and 0.02311 (-32.72 dB) for fault condition.

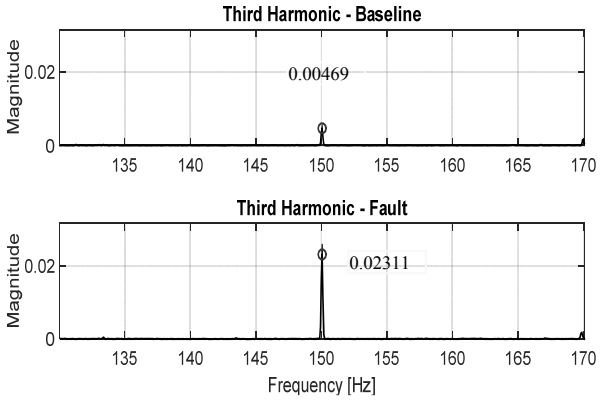

Figure 6. Third harmonic on current signature, for water fluid (stator electrical unbalance).

Regarding the EPVA electrical unbalance pattern, it is expected to be close to the 100 Hz frequency component on EPVA signature. From Fig. 7, the components magnitudes were 0.315% for baseline and 0.664% for fault condition. Thus, there was increase on both frequency magnitudes from baseline to fault condition, validating these fault patterns.

The second analyzed fault is mechanical misalignment. Fig. 8 presents the current spectra for the rotation frequency pattern. The first left and right sidebands of this fault patterns are expected to be close to the 33.333 Hz and 66.667 Hz frequency components, respectively. From Fig. 8, the components magnitudes were 0.01995 (-33.62 dB) (left) and 0.02960 (-30.09 dB) (right) for baseline and 0.03419 (-29.32 dB) (left) and 0.05007 (-26.01 dB) (right) for fault condition. There was increase on the analyzed frequency magnitudes from baseline to fault condition, which validates this fault pattern.

The last analyzed fault is mechanical unbalance. Fig. 9 presents the current spectra for the rotation frequency pattern. From Fig. 9, the components magnitudes were 0.01995 (-33.62 dB) (left) and 0.02960 (-30.09 dB) (right) for baseline and 0.02445 (-32.25 dB) (left) and 0.03643 (-28.78 dB) (right) for fault condition. There was a slight increase on the analyzed frequency magnitudes from

baseline to fault condition. This gives basis for the proposed fault pattern.

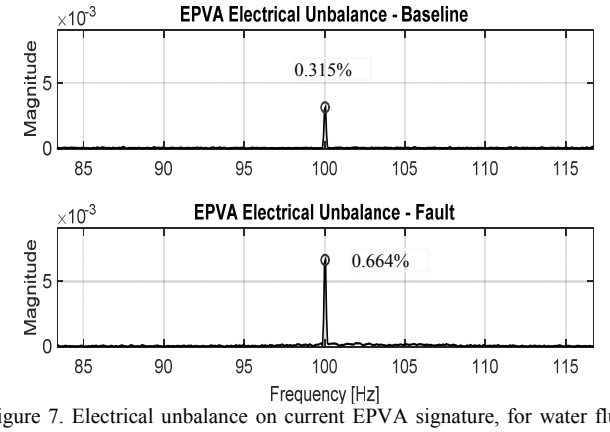

Figure 7. Electrical unbalance on current EPVA signature, for water fluid (stator electrical unbalance).

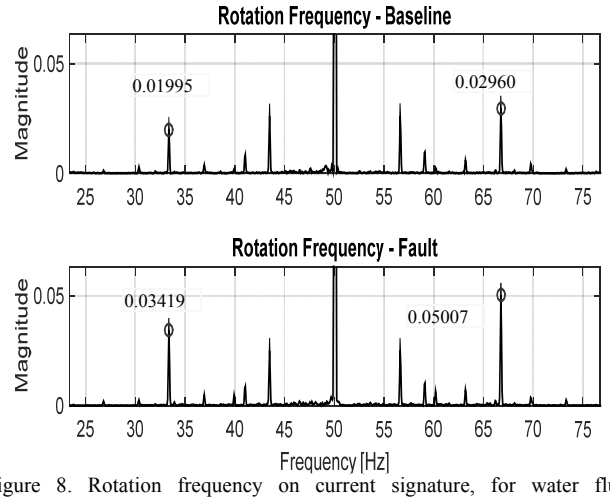

Figure 8. Rotation frequency on current signature, for water fluid (mechanical misalignment).

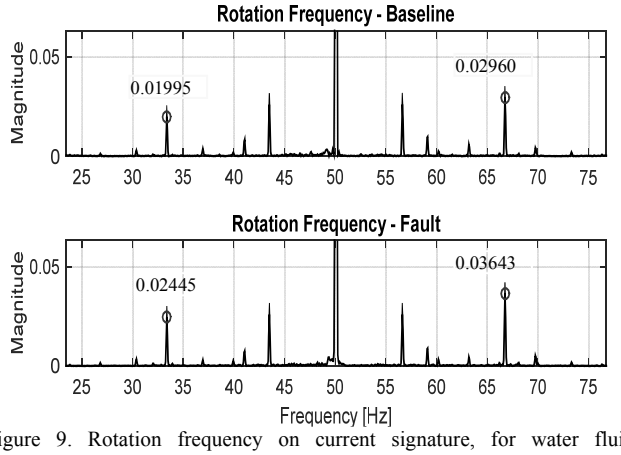

Figure 9. Rotation frequency on current signature, for water fluid (mechanical unbalance).

2. Diesel Fuel Fluid

For stator electrical unbalance, Figs. 10 and 11 present the current spectra for the third harmonic, and EPVA electrical unbalance fault patterns, respectively.

From Fig. 10, the third harmonic components magnitudes were 0.00362 (-48.82 dB) for baseline and 0.01723 (-35.28 dB) for fault condition. From Fig. 11, the EPVA electrical unbalance components magnitudes were 0.189% for baseline and 0.426% for fault condition. Thus, there was increase on both frequency magnitudes from baseline to fault condition, validating the analyzed fault patterns also for this type of fluid.

For mechanical misalignment, Fig. 12 presents the current spectra for the rotation frequency pattern. From Fig. 12, the components magnitudes were 0.01608 (-35.87 dB) (left) and 0.02720 (-31.31 dB) (right) for baseline and 0.03464 (-29.21 dB) (left) and 0.05780 (-24.76) dB (right) for fault condition. Thus, there was a significant increase on the analyzed frequency magnitudes from baseline to fault condition, validating this fault pattern.

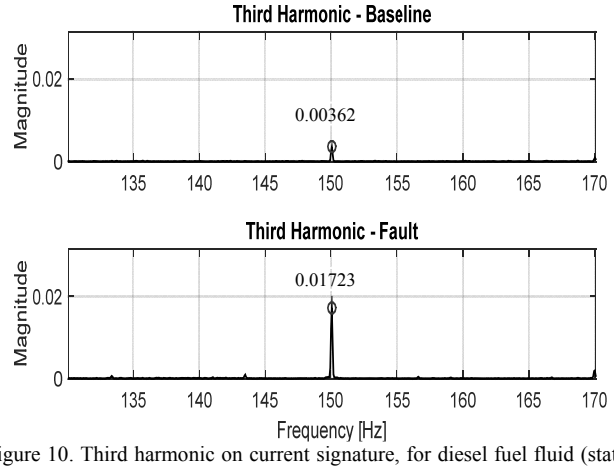

Figure 10. Third harmonic on current signature, for diesel fuel fluid (stator electrical unbalance).

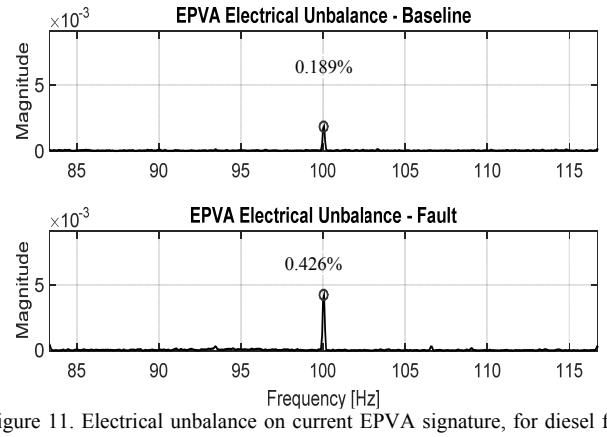

Figure 11. Electrical unbalance on current EPVA signature, for diesel fuel fluid (stator electrical unbalance).

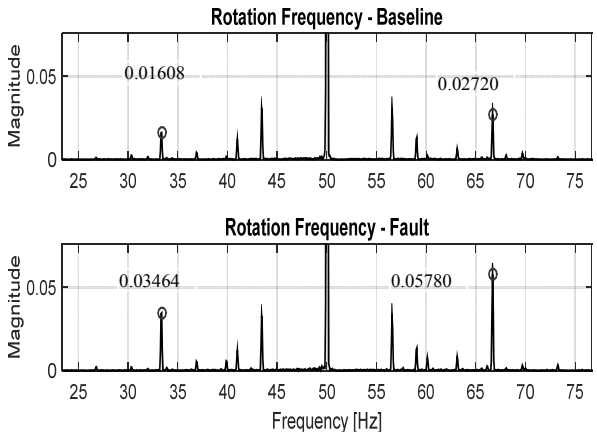

Figure 12. Rotation frequency on current signature, for diesel fuel fluid (mechanical misalignment).

For mechanical unbalance, Fig. 13 presents the current spectra for the rotation frequency pattern; where, the components magnitudes were 0.01608 (-35.87 dB) (left) and 0.02720 (-31.31 dB) (right) for baseline and 0.01848 (-34.66 dB) (left) and 0.03119 (-30.12 dB) (right) for fault condition. There was increase on the analyzed frequency magnitudes from baseline to fault condition. Thus, the fault pattern is validated.

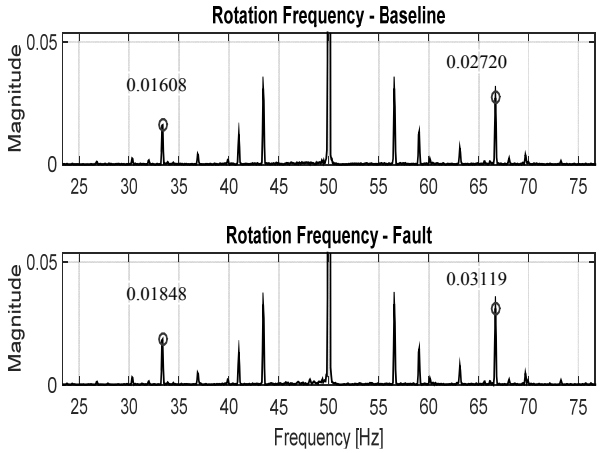

Figure 13. Rotation frequency on current signature, for diesel fuel fluid (mechanical unbalance).

3. Water plus Diesel Fuel Fluid

For stator electrical unbalance, Figs. 14 and 15 present the current spectra for the third harmonic, and EPVA electrical unbalance fault patterns, respectively, for baseline and fault conditions. From Fig. 14, the third harmonic components magnitudes were 0.00386 (-48.27 dB) for baseline and 0.01752 (-35.13 dB) for fault condition.

From Fig. 15, the EPVA electrical unbalance components magnitudes were 0.200% for baseline and 0.410% for fault condition. Thus, there was a significant increase on both frequency magnitudes from baseline to fault condition, which validates the analyzed fault patterns for this type of fluid. For mechanical misalignment, Fig. 16 presents the current spectra for the rotation frequency pattern. From Fig. 16, the components magnitudes were 0.01695 (-35.41 dB) (left) and 0.02838 (-30.94 dB) (right) for baseline and 0.04245 (-27.72 dB) (left) and 0.06977 (-23.25 dB) (right) for fault condition. Thus, there was a significant increase on the analyzed frequency magnitudes from baseline to fault condition, which validates this fault pattern for this fluid.

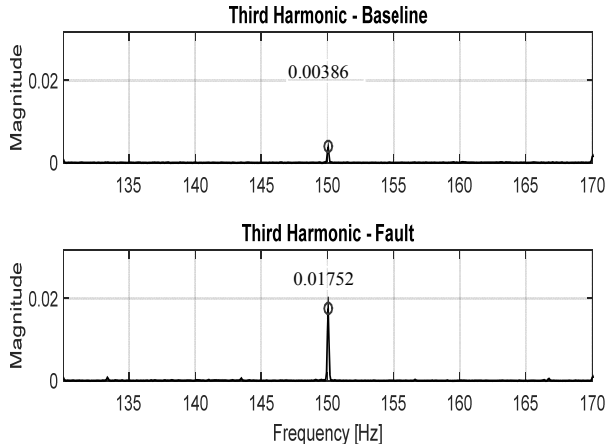

Figure 14. Third harmonic on current signature, for water plus diesel fuel fluid (stator electrical unbalance).

For mechanical unbalance, Fig. 17 presents the current spectra for the rotation frequency pattern. From Fig. 17, the components magnitudes were 0.01695 (-35.41 dB) (left) and 0.02838 (-30.94 dB) (right) for baseline and 0.02175 (-33.25 dB) (left) and 0.03665 (-28.72 dB) (right) for fault condition. There was a slight increase on the analyzed frequency magnitudes from baseline to fault condition. This gives basis for the proposed fault pattern.

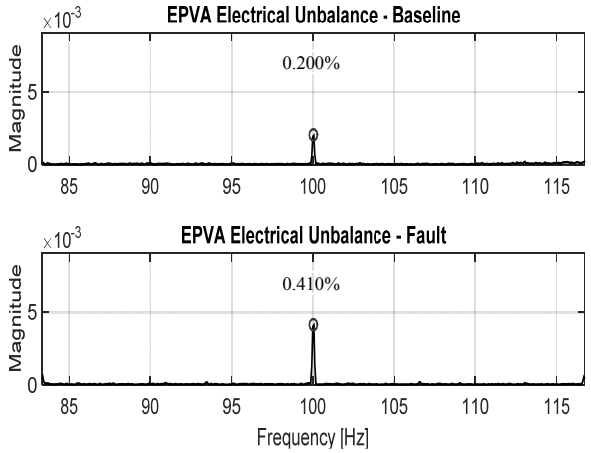

Figure 15. Electrical unbalance on current EPVA signature, for water plus diesel fuel fluid (stator electrical unbalance).

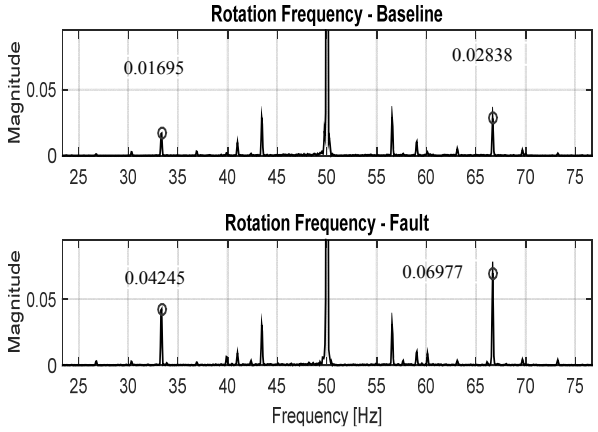

Figure 16. Rotation frequency on current signature, for water plus diesel fuel fluid (mechanical misalignment).

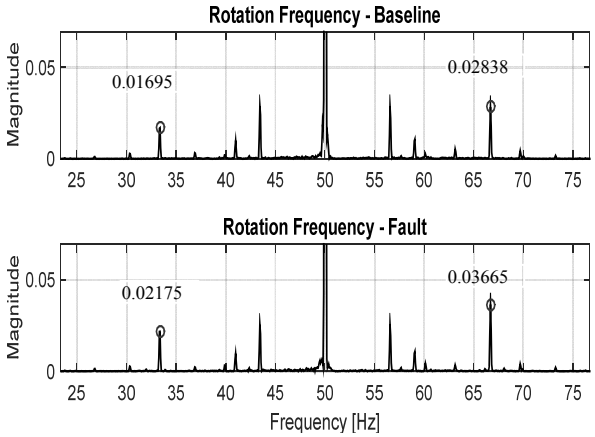

Figure 17. Rotation frequency on current signature, for water plus diesel fuel fluid (mechanical unbalance).

C. Final Comments

The fault patterns rely only on the line frequency and

structural characteristics of the machine. Thus, they are generic, and it is possible to infer that the results can be transferred to other systems and are valid for similar pump systems.

The only difference is related to the component magnitudes, which depend on the load condition, being specific for each machine. A common practice in PdM is to collect a data set at the time of the system installation and consider the magnitudes as the baseline. Then, in the continuous monitoring, if the magnitudes of the fault patterns suffer a considerable change, a fault may be developing in some part of the machine.

Another remark is that rotor rotation frequency is fault indicator for both mechanical misalignment and unbalance. This pattern is also related to mixed eccentricity. The nature of these faults is different, and the indicator can help the maintenance staff to search for a mechanical problem in the machine after ESA based diagnosis. The discrimination of both mechanical faults in this fault pattern can be studied in future works or can be achieved by analyzing other ESA fault patterns related to these faults, as presented in [6].

A final comment is that blurring may occur in the electrical signatures because of electrical and mechanical interactions and intrinsic characteristics of the measurement and acquisition system. However, these frequencies do not confuse the fault diagnosis by using ESA, because the analysis is comparative and the frequencies do not necessarily match fault pattern frequencies.

V. Conclusion

This paper presented a study on electrical signature analysis for PMSM condition monitoring. The study was accomplished by defining fault patterns on the current signature and performing experimental tests with a scale model laboratory. Preliminary experimental results for some simulated faults have been presented.

The results were promising, as the fault patterns have been validated for the three types of pumped fluids. Thus, the ESA allowed the faults detection considering the different load conditions of the PMSM. Moreover, some characteristics in the electrical signals have been identified, which can allow the fluid identification by analyzing the signals, which can be useful in some applications.

Finally, it is proposed for future works to deepen the study of electrical signature analysis for fault detection on PMSMs, including approaches to deal with speed variations and distinguish faults when the same fault patterns indicate more than one type of fault.

Acknowledgment

The authors would like to thank the National Council for Scientific and Technological Development (CNPq), Coordination for the Improvement of Higher Education Personnel (CAPES), and the Brazilian Electricity Regulatory Agency Research and Development (ANEEL R&D) for supporting this project.

References

[1] D. Reljic, D. Jerkan, D. Marcetic, Dj. Oros, “Broken bar fault detection in IM operating under no-load condition,” Advances in Electrical and Computer Engineering, vol. 16, no. 4, pp. 63-70, 2016, doi: 10.4316/AECE.2016.04010.

[2] A. G. Espinosa, J. A. Rosero, J. Cusidó, L. Romeral, J. A. Ortega, “Fault detection by means of Hilbert-Huang transform of the stator current in a PMSM with demagnetization,” IEEE Transactions on Energy Conversion, vol.25, no.2, pp.312–318, June 2010, doi: 10.1109/TEC.2009.2037922.

[3] J. C. Urresty, J. R. Riba, L. Romeral, “Diagnosis of interturn faults in PMSMs operating under nonstationary conditions by applying order tracking filtering,” IEEE Transactions on Power Electronics, vol.28, no.1, pp.507–515, Jan 2013, doi: 10.1109/TPEL.2012.2198077.

[4] H. Saavedra, J. R. Riba, L. Romeral, “Detection of inter-turn faults in five-phase permanent magnet synchronous motors,” Advances in Electrical and Computer Engineering, vol.14, no.4, pp.49-54, 2014, doi: 10.4316/AECE.2014.04008.

[5] D. Matic, Z. Kanovic, "Vibration based broken bar detection in induction machine for low load conditions," Advances in Electrical and Computer Engineering, vol.17, no.1, pp.49-54, 2017, doi:10.4316/AECE.2017.01007.

[6] E. L. Bonaldi, L. E. L. de Oliveira, J. G. Borges da Silva, G. Lambert-Torres, L. E. Borges da Silva, “Predictive maintenance by electrical signature analysis to induction motors,” in Induction Motors—Modelling and Control, Rui Araujo, Eds., Rijeka, Croatia: InTech, 2012, pp.487–520, ISBN 978–953-51-0843-6, doi: 10.5772/48045.

[7] C. P. Salomon, W.C. Santana, G. Lambert-Torres; L. E. Borges da Silva, E. L. Bonaldi, L. E. de Oliveira, J. G. Borges da Silva, A. L. Pellicel, G. C. Figueiredo, M. A. A. Lopes, “Discrimination of Synchronous Machines Rotor Faults in Electrical Signature Analysis based on Symmetrical Components,” IEEE Transactions on Industry Applications, vol.53, no.3, pp.3146-3155, May/June 2017, doi: 10.1109/TIA.2016.2613501.

[8] J. Hang, J. Zhang, M. Cheng, S. Ding, “Detection and discrimination of open-phase fault in permanent magnet synchronous motor drive system,” IEEE Transactions on Power Electronics, vol.31, no.7, pp.4697–4709, July 2016, doi: 10.1109/TPEL.2015. 2479399.

[9] J. A. Rosero, L. Romeral, J. Cusido, A. Garcia, J. A. Ortega, “On the shortcircuiting fault detection in a PMSM by means of stator current transformations,” Proc. 2007 IEEE Power Electronics Specialists Conference, IEEE PESC 2007, Orlando, pp.1936–1941, June 2007, doi: 10.1109/PESC.2007.4342300.

[10] T. Boileau, N. Leboeuf, B. Nahid-Mobarakeh, F. Meibody-Tabar, “Stator winding inter-turn fault detection using control voltages demodulation,” Proc. 2012 IEEE Transportation Electrification Conference and Expo, IEEE ITEC 2012, Dearborn, pp.1–6, June 2012, doi: 10.1109/ITEC.2012.6243477.

[11] J. C. Urresty, J. R. Riba, L. Romeral, “Influence of the stator windings configuration in the currents and zero-sequence voltage harmonics in permanent magnet synchronous motors with demagnetization faults,” IEEE Transactions on Magnetics, vol.49, no.8, pp.4885–4893, Aug 2013, doi: 10.1109/TMAG.2013.2247046.

[12] J. Hang, J. Zhang, M. Cheng, Z. Wang, “Fault diagnosis of mechanical unbalance for permanent magnet synchronous motor drive system under nonstationary condition,” Proc. 2013 IEEE Energy Conversion Congress and Exposition, IEEE ECCE 2013, Denver, pp.3556–3562, Sept 2013, doi: 10.1109/ECCE.2013.6647169.

[13] W. le Roux, R. G. Harley, T. G. Habetler, “Detecting Rotor Faults in Low Power Permanent Magnet Synchronous Machines,” IEEE Transactions on Power Electronics, vol.22, no.1, pp.322-328, 2007, doi: 10.1109/TPEL.2006.886620.

[14] B. M. Ebrahimi, M. Javan Roshtkhari, J. Faiz, S. V. Khatami, “Advanced Eccentricity Fault Recognition in Permanent Magnet Synchronous Motors Using Stator Current Signature Analysis,” IEEE Transactions on Industrial Electronics, vol.61, no.4, pp.2041-2052, April 2014, doi: 10.1109/TIE.2013.2263777.

[15] J. Rosero, J. L. Romeral, J. Cusido, J. A. Ortega, A. Garcia, “Fault detection of eccentricity and bearing damage in a PMSM by means of wavelet transforms decomposition of the stator current,” Proc. 2008 Twenty-Third Annual IEEE Applied Power Electronics Conference and Exposition, IEEE APEC 2008, Austin, pp.111-116, Feb. 2008, doi: 10.1109/APEC.2008.4522708.

[16] C. P. Salomon, W. C. Santana, G. Lambert-Torres, L. E. Borges da Silva, E. L. Bonaldi, L. E. L. de Oliveira, “Comparison among Methods for Induction Motor Low-Intrusive Efficiency Evaluation Including a New AGT Approach with a Modified Stator Resistance”, Energies, vol.11, no.4, pp.691-712, April 2018, doi: 10.3390/en11040691.

[17] J. R. Cameron, W. T. Thomson, A. B. Dow, “Vibration and current monitoring for detecting airgap eccentricity in large induction motors,” IEE Proceedings B - Electric Power Applications, vol.133, no.3, pp.155–163, May 1986, doi: 10.1049/ip-b.1986.0022.

[18] J. Sottile, F. C. Trutt, A. W. Leedy, "Condition monitoring of brushless three-phase synchronous generators with stator winding or rotor circuit deterioration," IEEE Transactions on Industry Applications, vol.42, no.5, pp.1209–1215, Sep./Oct. 2006, doi: 10.1109/TIA.2006.880831.

[19] S. M. A. Cruz, A. J. M. Cardoso, "Stator winding fault diagnosis in three-phase synchronous and asynchronous motors, by the extended park's vector approach," IEEE Transactions on Industry Applications vol.37, no.5, pp.1227–1233, Sep./Oct. 2001, doi: 10.1109/28.952496.